Scaled experiments using the helium technique to study the vehicular blockage effect on longitudinal ventilation control in tunnels

Alva, Wilson Ulises Rojas; Jomaas, Grunde; Dederichs, Anne

Published in:
Proceedings of the 16th International Symposium on Aerodynamics, Ventilation & Fire in Tunnels

Publication date:
2015

Document Version
Peer reviewed version

Scaled experiments using the helium technique to study the vehicular blockage effect on longitudinal ventilation control in tunnels

W U Rojas Alva, G Jomaas, A S Dederichs
Civil Engineering Department, Technical University of Denmark, Denmark

ABSTRACT

A model tunnel (1:30 compared to a standard tunnel section) with a helium-air smoke mixture was used to study the vehicular blockage effect on longitudinal ventilation smoke control. The experimental results showed excellent agreement with full-scale data and confirmed that the critical velocity decreases in proportion with the blockage ratio. Nevertheless, it was found that the relative position of the fire source and the relative size of the vehicular blockage can have an opposite effect, as the vehicular blockage influenced the critical and confinement velocity. The method demonstrated the ability to provide valuable information on the effect of vehicular blockage on tunnel fire dynamics.

NOMENCLATURE

A	Cross section area of the tunnel [m^2]	$\hat{L}$	Thermal-densimetric scale relationship
A_{Local}	Local area of the vehicular blockage [m^2]	l	Backlayering distance [m]
C_p	Specific heat capacity of air [J/kgK]	l^*	Dimensionless backlayering distance
g	Gravitational acceleration [m^2/ s]	$\dot{m}$	Mass burning rate [kg/m^2/s]
H	Tunnel height [m]	n	Air entrainment ratio
k	Dimensionless coefficient	$\dot{Q}$	Heat release rate [kW]
L	Scale relationship	$\dot{Q}_c$	Convective heat release rate [kW]
q_s	Smoke volume flow rate [m^3/s]	V_c	Critical velocity [m/s]
q_{air}	Smoke volume flow rate of air [l/min]	V_c^*	Dimensionless critical velocity
q_{he}	Smoke volume flow rate of helium [l/min]	V_{ctr}^*	Dimensionless critical velocity with vehicular blockage
R	Heptane pool radius [m]	V^{**}	Confinement velocity
S	Heptane pool area [m^2]	V_{tr}^{**}	Confinement velocity with vehicular blockage
T_0	Ambient temperature [K]	z	Height above the pool [m]
T_s	Smoke temperature [K]	X_{air}	Mass fraction rate of air [%]
V	Longitudinal ventilation velocity [m/s]	X_{he}	Mass fraction rate of helium [%]
V^*	Dimensionless ventilation velocity [m/s]	X_r	Radiative fraction [%]

Greek letters

ΔH_c	Heat of combustion [J/kg]
ΔT	Temperature difference between the hot gases and the surrounding air
$\Delta\rho$	Temperature difference between the hot gases and the surrounding air
ρ_{air}	Air density [kg/m^3]
ρ_{he}	Helium density [kg/m^3]
φ	Tunnel blockage ratio

Subscripts

m	Model scale
f	Full scale
th	Thermal similarity
ρ	Densimetric similarity

1. INTRODUCTION

Catastrophic fire disasters in tunnels [1–3] have been demonstrated that the smoke represents the largest risk for people present in the tunnel during a fire. Therefore, any potential smoke release in a tunnel is now controlled either by longitudinal or a transversal smoke control system [4], with the former being most extensively applied. In the event of a fire in a tunnel, by diverse reasons, the combustion process from the fire source will rapidly generate a buoyant plume of smoke that will impinge the tunnel's ceiling and the smoke will thus travel downstream and upstream from the fire source, covering the tunnel section. The ventilation system is then activated and the jet fans will push the smoke with certain "longitudinal velocity" in one direction towards one of the portals (downstream) in order to prevent the smoke traveling upstream from the fire source. The extent of the upstream travel is called the "backlayering distance", and when the backlayering distance disappears, the applied flow from the smoke control system is said to have reached the "critical velocity". As a result, one side of the tunnel (as seen from the location of the fire) is kept free of smoke and tenable criteria are met for occupants. Nevertheless, the other side of the tunnel can be completely covered by smoke due to the (turbulent) flow from the smoke control system.

When longitudinal ventilation is applied with the critical velocity, a large amount of oxygen is transported to the fire, and the fire will grow and more smoke will be produced. This smoke will be non-stratified, and thus has the potential to jeopardize tunnel occupants located downstream of the fire source [5]. This hazard can be reduced if certain backlayering distance is allowed and at the same time smoke stratification downstream of the fire source is preserved. The corresponding minimum longitudinal velocity is typically referred to as the "confinement velocity" [6].

Scaling is not a novel method; it was already used in 1906 to investigate the Austrian Theatre disaster [7]. Three methods are common, namely Froude modelling, Analogue modelling and pressure modelling. The critical velocity has been studied in detail [8–18] using the scaling techniques as well as through full scale measurements and many correlation have been drawn to quantify it. The backlayering distance has been reported [8,12,19–21], but to a lesser extent. Most previous studies assumed that the tunnel was free of obstacles or had no presence of other vehicles in the vicinity of the fire source. As such, few studies have been conducted in order to understand and quantify the effect of vehicular blockage on the critical velocity, backlayering distance or the confinement velocity [21–23]. Furthermore, the few studies conducted were not parametric-based. Thus, there is clearly still a knowledge gap regarding the effect of the vehicular blockage on the longitudinal ventilation control. Therefore, a set of experiments were conducted in a model tunnel (scale 1/30) in order to study the effect of the vehicular blockage under several parametric conditions considering different tunnel sections, several blockage

ratios, different heat release rates and the relative position of the fire source. The investigation was based on air-helium technique developed by Vauquelin & Mégret [24–26].

In the next chapters an overview of the key correlations are presented together with the theoretical background used for this study. This is followed by an explanation of the experimental procedure and finally the results are compared to full scale data and the experimental results are discussed before the conclusion to the study is drawn.

2. CRITICAL VELOCITY, BACKLAYERING DISTANCE AND VEHICULAR BLOCKAGE

The first attempt to correlate the critical velocity and backlayering distance was made by Thomas [8,7] where he studied the movement of buoyant flows, caused by a fire, against an induced air flow in horizontal passages. He performed experiments in a 90 x 90 cm wind tunnel at 1/40 scale, the results showed that a minimum air velocity was required to prevent backlayering distance upwards from the fire source, or critical velocity. Based on the data, the critical velocity was found to be correlated to one third power of the heat release rate. As the Froude modelling approach was applied [27], only buoyancy forces, viscous forces and Reynolds number were conserved. Thomas found [8,7] that the gas flow pattern or backlayering distance can only be a function of the ratio buoyancy and inertial forces in the tunnel section; this ratio is expressed as the critical Froude number [21]. Thomas suggested that the critical Froude number is equal to unity when the energy from the incoming fresh air has to balance the energy of the buoyant source at critical conditions, causing the backlayering distance disappears. However, Li et al. [21] found that the critical Froude number is a function of the dimensionless heat release rate, which implies that the critical Froude number varies contrarily to the constant critical Froude number suggested by Thomas.

Thomas proposed the following correlation for the critical velocity:

$$V_c = k\left(\frac{g\dot{Q}_c}{\rho_0 C_p T_0}\right)^{1/3} \tag{1}$$

Where k is a coefficient and it was found to be equal to the unity only for the corresponding experimental set-up. Thomas also proposed a correlation for the backlayering distance based on a theoretical approach:

$$l^* = \frac{l}{H} = \frac{gHQ}{\rho_0 C_p T_0 V^3 A} \tag{2}$$

Oka & Atkinson [13] studied the critical velocity in a model tunnel with propane gas as the fire source under several parametric conditions such the fire source shape, fire source location, and the fire size ranging from 2 to 150 MW. This was the first time that blockage in the tunnel section was studied. They found that when the tunnel is partly blocked the critical velocity is affected and thus it is diminished, this can be explained by the fact that the blockage reduces the air entrainment to the fire source, thus decreasing the burning and the fire size. Based on the results it was found that when the blockage object occupies 12% of the tunnel section the critical velocity decreases approximately 15%, and when the object occupies 32% of the tunnel section the critical velocity is

reduced approximately 40-50%. The data however could have been influenced by the cooling system, the walls in the vicinity of the fire source were cooled down with water during the execution of the experiments, furthermore only one section was studied, the colliery arch.

Vauquelin & Telle [20] studied the longitudinal velocity which is induced in a tunnel owing to smoke extraction throughout the extraction vents located at the ceiling level. For the first time the term "Confinement velocity" was introduced and applied when the backlayering distance is less than 4 times the tunnel height upstream at the extraction vent; however only for transversal ventilation system. In another study a dimensionless confinement velocity in longitudinal ventilations systems was introduced by Li et al. [21]. They carried out experimental and theoretical analysis in order to study the critical velocity, backlayering distance and confinement velocity with or without presence of vehicle obstruction. Small scale test were conducted in two tunnel sections, and a model train vehicle was place inside one of the tunnels on top of the fire source and 40 mm above the tunnel floor, the blockage occupied 20% of the tunnel's section. Based on the dimensional analysis and experimental results, Li et al. [21] proposed the following correlations for the critical velocity without and with vehicular blockage respectively:

$$V_c^* = \begin{cases} 0.81Q^{*1/3}, & Q^* \le 0.15 \\ 0.43, & Q^* > 0.15 \end{cases} \tag{3}$$

$$V_{ctr}^* = \begin{cases} 0.63Q^{*1/3}, & Q^* \le 0.15 \\ 0.33, & Q^* > 0.15 \end{cases} \tag{4}$$

Where Q^* and V_c^* are the dimensionless heat release rate and the dimensionless critical velocity respectively.

$$Q^* = \frac{Q}{\rho_0 C_p T_0 g^{1/2} H^{5/2}} \tag{5}$$

$$V_c^* = \frac{V_c}{\sqrt{gH}} \tag{6}$$

They defined confinement velocity in dimensionless form, V^{**}, as function of the longitudinal velocity, V, and its corresponding critical velocity, V_c :

$$V^{**} = \frac{V^*}{V_c^*} = \frac{V}{V_c} \tag{7}$$

The dimensionless backlayering distance was found to be a function of the confinement velocity. They proposed the following empirical correlation without vehicular blockage and with vehicular blockage respectively:

$$V^{**} = \exp\left(-0.054 l^*\right) \tag{8}$$

$$V_{tr}^{**} = \exp\left(-0.074 l^*\right) \tag{9}$$

The proposed correlations for the critical velocity and backlayering distance are in agreement with full-scale experimental data. Oka & Atkinson [13] found similar results with respect to the critical velocity with vehicular blockage. Even though there is no full-scale data for backlayering distance when there is vehicular blockage, they concluded that the vehicular blockage has a significant impact on both the critical velocity and the backlayering distance. It has to be noted that the proposed formulae are based solely on one tunnel section and one blocking vehicle.

Li et al. [22] conducted numerical studies using FDS version 5.5 with respect to the effect of vehicular blockage on the critical velocity in a tunnel fire event. The tunnel case was the same as used by Li et al. [21] and the fire source was located on top of the vehicular blockage. They defined the tune blockage ratio, φ , as the ratio of the cross-sectional area of the fire source to the cross-sectional area of the tunnel. Thus the local open area is:

$$A_{local}=A(1-\varphi) \tag{10}$$

Based on the numerical and small-scale data, they proposed the following correlation, where the effect of the blockage ratio is included:

$$V_{ctr}=V_c(1-\varphi) \tag{11}$$

The FDS results showed a ±15% relative error for the critical velocity when compared with the experimental data from other small scale results. Lee & Tsai [23] proposed the same relationship, equation (11), they executed small-scale experiments and numerical simulations in order to investigate the effects of vehicular blockage on the tunnel fire behaviour and critical velocity in tunnel with longitudinal ventilation scheme. The studied scenarios comprised two tunnel cross sections, three vehicular blockage models into two or three arrays and, with a blockage ratio in the range 5 to 31 % and different fire source locations. The fire source was simulated with small gasoline pools fire placed in pans and the fire source was ranged between 5 and 10 MW. Based on the experimental data Lee & Tsai [23] concluded that the critical velocity is affected by the vehicular blockage in the same range as the vehicular blockage, however they observed that the relative position of the fire source can have the opposite effect. Due to lack of further analysis the data obtained by Lee & Tsai is further analysed herein, along with the current results.

3. METHOD

3.1 The scaling principles

The reproduction of different phenomena and parameters from a full-scale fire to a densimetric small-scale fire, see Figure 1, involves two groups of scaling principles based on physical analogies, which are dynamic similarities and thermal/densimetric similarities [26]; a collection of formulae based on a semi-empirical model [24] in order to quantify the involved parameters; and finally the equivalence of smoke flow rate to a gas densimetric buoyant mixture of helium-air [25].

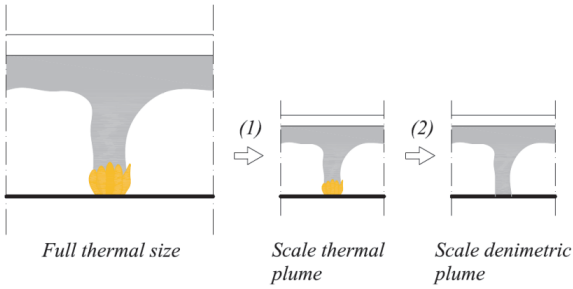

Figure 1 – Principle of the two step-scaling, [28]**.**

Based on Froude modelling, the scaling of flow equations implies the conservation of the three non-dimensional groups [25,26], referred as: the Reynolds number, which is the ratio between inertial forces and viscosity forces. The Reynolds number is difficult to preserve but if kept sufficient high ensures a minimum turbulent flow. The Froude number, which is the ratio between inertial forces and buoyancy forces, It has to be preserved in order to reproduce the buoyancy effect and stratification. Finally the Prandtl number, which is the ratio of thermal to motion diffusivity, it is always preserved due its non-dependency to the tunnel geometry. The scaling relationships between the model ($_m$) and full size ($_f$) for the length, velocity and volumetric flow rate are respectively:

$$L=L_m/L_f\,,\qquad V_m=L^{1/2}V_f,\qquad q_m=L^{5/2}q_f \tag{12}$$

Vauquelin & Mégret [25,26] established a thermal/densimetric analogy in order to describe the analogue characteristics between a real plume and a light mixture jet, thereby they stablished further similarity laws. In a real fire, the thermal plume is generated by the overheating of the fluid particles into the flame at temperature $T=T_0+\Delta T$, issued at the thermal velocity V_{th}. On the contrary, the physical model simulates the corresponding flow with a densimetric plume at ambient temperature T_0, where the flow depends on the relative density difference $\Delta\rho/\rho$ and the injection velocity V_ρ. The non-dimensional groups must be ensured as in the previous dynamic similarity. In this case the Reynolds number and densimetric Froude number are preserved, and the preservation of the Prandtl number (thermal plume) is identified with the Schmidt number in terms of diffusivity (densimetric plume). A link was introduced between the thermal and densimetric plumes [25,26], and the length ratio $\hat{L}$. Thus the following scaling relationships are imposed:

$$\hat{L}=L_{th}/L_\rho\,,\ u_\rho=\hat{L}u_{th},\ \frac{\Delta\rho}{\rho}=\hat{L}^3\frac{\Delta T}{T_0},\ q_\rho=\frac{1}{\hat{L}}q_{th} \tag{13}$$

Two dimensionless factors L and $\hat{L}$ can allow a mathematical link between the thermal and the densimetric flows. According to Vauquelin & Mégret [26] the geometric scale ratio is easily implemented, but the length ratio $\hat{L}$ is of major interest inasmuch as it allows to simulate a real fire with a densimetric gas mixture of helium and air and it requires changes in the geometrical scale. Nonetheless in the case with the same temperature rise during execution of experiments, solely one value of $\hat{L}$ is required, and thus it can be taken as unity.

In order to apply the aforementioned similarity rules, several physical parameters have to be quantified. In order to achieve this goal a semi-empirical model developed by

Vauquelin & Mégret [24] is used to evaluate tunnel fire characteristics. Such a model was validated against full-scale data and its validity is applicable for heat release rates up to 50-60 MW. The model is based on a heptane pool fires and the following correlations are explained briefly:

$$\dot{Q}_c=(1-X_r)\dot{m}S\Delta H_c=(1-X_r)\dot{Q} \tag{14}$$

The air entrainment ratio, n, is the amount of air entrained by natural convection supplied to the stoichiometric proportion of air required to the complete combustion. Koseki & Yumoto [29] gave the following empirical correlation between air entrainment ratio and height above the pool, this correlation is only valid for pool fire from 0.6 to 16 m.

$$n=11\left[2.13\left(\frac{z}{R}\right)^{0.53}-1\right],\ \text{with } z/R>0.5 \tag{15}$$

If the air entrainment ratio at the ceiling level is known, no air entrainment is considered in the plume before reaching the tunnel ceiling, since the tunnel height is relatively small to the tunnel length. Then the smoke temperature can be estimated by the following second-order polynomial correlation, which is dependent on air entrainment and it takes only the convective heat.

$$(30.7+2n)10^{-3}T_s^2+(407+32.7n)T_s-\left(8.77\ 10^5+9.9\ 10^3 n\right)=0 \tag{16}$$

The following correlation predicts the smoke volume flow rate, taking into account the expansion effect owing to hot gases, at the tunnel ceiling level, the pool diameter, air entrainment ratio and smoke temperature.

$$q_s=(13.8+1.2n)S\dot{m}\frac{T_s}{T_0} \tag{17}$$

By applying the scaling relationships to the smoke flow rate, see equation (12), the corresponding smoke flow in reduced scale can be estimated. The corresponding air and helium mass fractions define the proportion of the respective flow to assure a certain total flow rate that can effectively reproduce a hot buoyant plume into a densimetric buoyant mixture. The mass fractions relations for helium and air are respectively:

$$\begin{cases} X_{he}=\dfrac{\rho_{air}}{\rho_{air}-\rho_{he}}\dfrac{\Delta T}{T_0+\Delta T} \\ X_{air}=1-X_{he} \end{cases} \tag{18}$$

Finally the corresponding helium and air volume flow rates can be determined by:

$$\begin{cases} q_{he}=X_{he}q_m \\ q_{air}=X_{air}q_m \end{cases} \tag{19}$$

3.2 The experimental procedure

A 4.65 m long model tunnel was designed with the main purpose to allow the simulation of a fire by means of releasing a buoyant jet of a helium-air mixture into a channel and make possible the measurement and characterisation of the phenomena involved in order to control the smoke by means of longitudinal scheme. The experimental rig has the

following characteristics: possibility of a great modularity of the tunnel section, thus the dimensions are changeable. This allows for visualisation of the buoyant jet, and thereby the backlayering distance can be quantified, the longitudinal velocities can be measured easily. Furthermore, it allows a wide range of heat release rates, it allows the presence of vehicular blockage, and it allows repeatability of experiments.

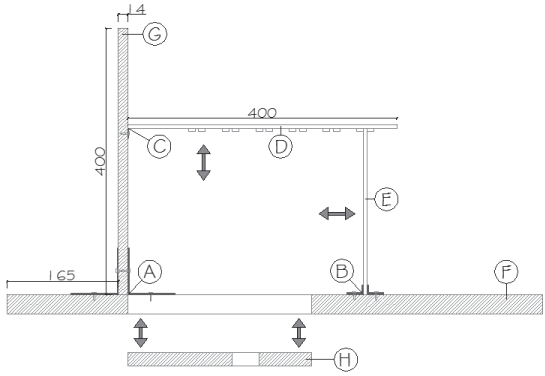

Figure 2 – Model tunnel cross section, principle of the modular geometry.

The tunnel model section can be seen in Figure 2 where the fixed wall (G) and the based (F) are made of wooden, the several movable walls (E) and the ceiling (D) are made of Plexiglas. The last pieces are movable and allow the modularity of tunnel dimensions. The source of injection requires different diameters due to the heptane pool semi-empirical model, thus several traps (H) are tailored with different diameter sources and it can be placed in the middle of the tunnel length.

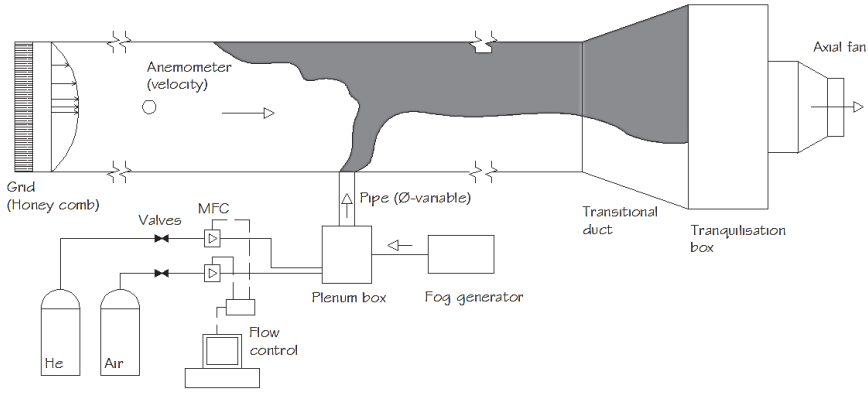

Figure 3 – Schematic of the experimental rig (not to scale).

The buoyant jet is a mixture of air and helium gases which are supplied at different flow rates depending on the heptane pool fire size. The gases are supplied from 50 l cylinders and regulated by means of Bronkhorst mass flow controllers (MFC), one MFC can regulate the air flow from 4.4 to 220 l/min and the other can regulate the helium flow from 10.8 to 540 l/min. Inasmuch as the buoyant mixture is colourless, it was seeded in the plenum box with mineral oil particles emitted form a fog generator model Antari Z-1500II, see Figure 3. The longitudinal ventilation system was achieved by extracting the seeded buoyant mixture from one end of the tunnel model; an axial fan K100M with a

maximum air flow of 163 m^3/h was located at one end of the model after a transitional duct and a tranquilisation box. The longitudinal flow in the tunnel was regulated with a potentiometer, thus several longitudinal velocities could be achieved. The longitudinal air velocity was measured several points of the cross section located at 0.88 m. from the fire source, then an average value was estimated for the corresponding longitudinal air velocity, an anemometer Kimo VT100E was used for the air velocity measurements.

Table 1 – An overview of conducted experiments for several scenarios.

Scenarios	SET 1				SET 2									SET 3					
Dimension	[9x6m]				Variable Width [m]									Variable Height [m]					
					4.5			7.5		10.5				4.5				10.5	
Vehicular blockage	w.			wo.	w.			wo.	wo.	w.			wo.	w.			wo.	w.	wo.
HRR [MW]	a1	b1	c1		a2	b2	c2			a2'	b2'	c2'		a3	b3	c3		c3'	
0.42				xx				x	x				x				x		X
0.78				xx	zz	z	yy	xx	xx	zz	y		xx	yy	zz		xx		Xx
0.96	yy	zz	yy	xx														yy	Xx
1.61				xx	zz	zz		xx	xx			yy	xx			yy	xx	yy	X
2.62	yy		yy	xx			zz	xx	x			y	xx						X
5.28				xx					x				x				x		X
6.85		zz	y	xx															
9.60				xx															
13.61				xx															
16.24				xx															
26.16[1]																	x		
30.87[1]																	x		

A detailed matrix of all the experiments can be seen in Table 1, which shows that there are three main sets of experiments (further information on the experiments can be found in Table A1 in the appendix). In the first set the dimensions of the model tunnel were fixed simulating standard tunnel dimensions of 9 m. width and 6 m. height in full-scale. In the second set one of the dimensions, the width, was variable and the height fixed to 6 m. and finally in the third set the height was the varying dimension. Several HRR were studied considering corresponding values of standard vehicle sizes, like passenger cars and lorries [4], the abbreviates "w." and "wo" stand for experiments with and without presence of vehicular blockage respectively.

The experiments without vehicular blockage were aimed to validate the data against full-scale measurements. Three types of vehicular blockage were considered with different arrays according to each scenario, the scaled vehicles were a normal car (a) with dimensions of 1.86 x 1.5 x 4.5 m. in full-scale, a bus (b) with dimensions 2.34 x 2.97 x 11.4 m. and a train (c) with dimensions 3 x 3.69 x 17.4 m. Consequently several blockage ratios were achieved ranging from 10.3 to 41 %. The experiments that correspond to tunnel without vehicular blockage are identified by "x", one "x" means that only critical velocity was measured for that experiment, two "xx" means that critical velocity and backlayering distance was measured for that experiment and for these experiments the

[1] These values correspond to 1/40 scale tunnel, the scale was further reduced since the mass flow controllers did not allow higher air and helium flow rates, thus larger HRR could be reached.

fire source was located anywhere on the floor, so to say in the centre or close to the tunnel´s wall. In the case of experiments with vehicular blockage identified by one or two "y", as in the previous case both parameters were measured, but the fire source was located downstream of the fire source right after the vehicular blockage. On the contrary if the fire source was not located downstream of the vehicular blockage, then it is identified by "z".

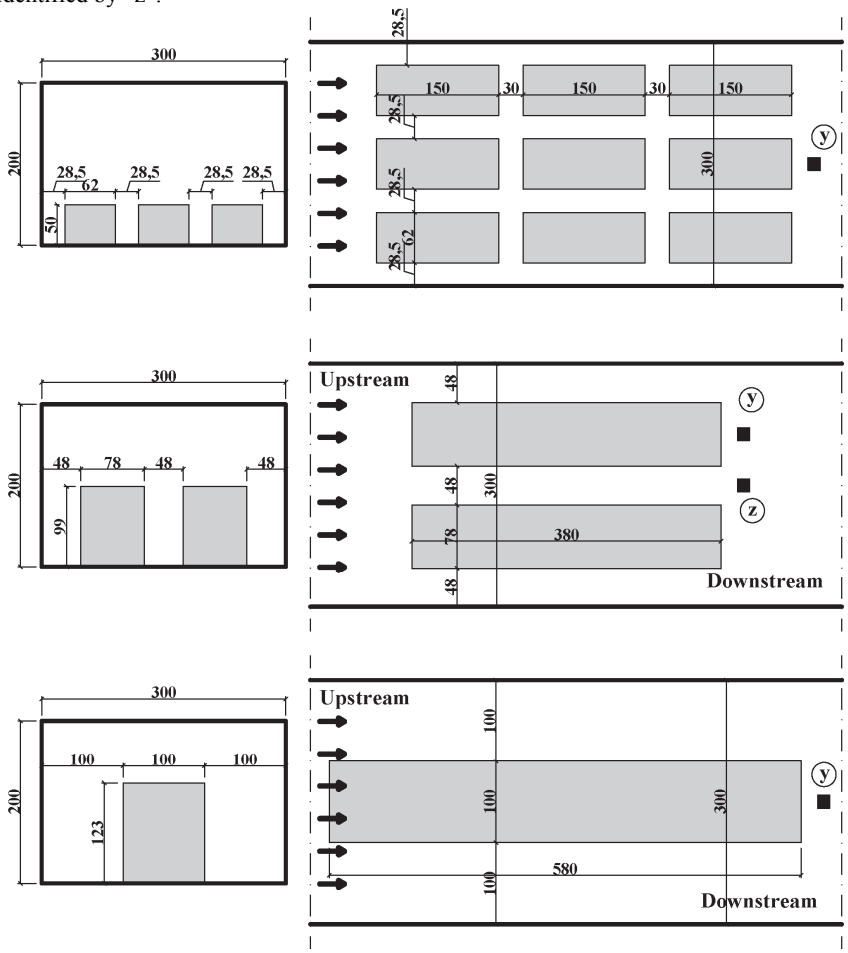

Figure 4 – Vehicular blockage models, A, B and C and fire source locations for scenarios set 1.

4. RESULTS

The overall results from all sets that correspond to the critical velocity without blockage ratio are translated into dimensionless form and plotted in Figure 5 together with full-scale data from the Memorial tunnel fire tests [30], the Runehamar tunnel fire tests [30], the EUREKA program [14] and Buxton [14], as well as from a correlation, see equation (3), proposed by Li et al. [21]. It is observed that the obtained results are in good agreement with the correlation and data from full-scale experiments and it can be seen that some results indicate slightly the asymptotic behaviour, and for small dimensionless

heat release rate the obtained results show that the dimensionless critical velocity is slightly over estimated. This might be due to the seeding system used in order to colour the buoyant mixture, the fog generator release the oil particles with a small trust, although this was minimised.

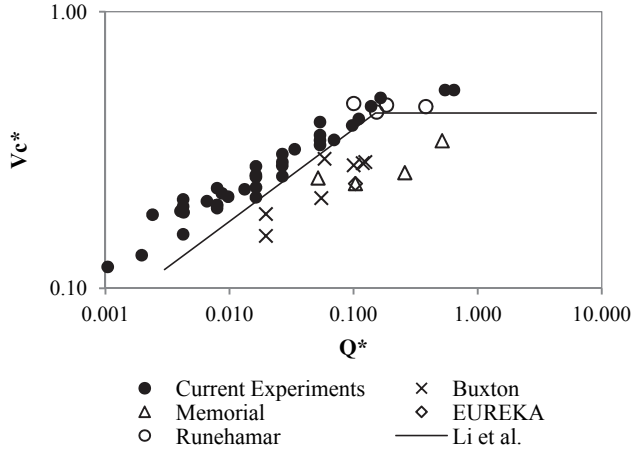

Figure 5 – Dimensionless critical velocity as a function of the dimensionless heat release rate. Overall results compared against full-scale data and a correlation Li et al. [21]**.**

The data concerning the critical velocity according to the relative position of the fire source are plotted in Figure 6 for the experimental data and in Figure 7 for the data by Lee & Tsai [23] data. Both graphs display results from the correlation proposed by Li et al. [22]. From both figures it is clear that the data that corresponds to the fire position located downstream of the vehicular blockages does not follow the reference correlation. On the contrary the data which corresponds to the fire position not located downstream of the vehicular blockage do follow and lie close to the reference correlation. Based on the data presented for blockage ratio, two main comments can be brought up. When there is presence of vehicular blockage in the tunnel model and the longitudinal air stream reaches directly the fire plume, isothermal or thermal, the critical velocity decreases following the correlation proposed by Li et al. [22] but when the fire plume is partly blocked and the longitudinal air stream does not reach it, then the critical velocity does not follow the reference correlation.

The fire plume or buoyant jet is affected by the vehicular blockage. When there is no vehicular blockage, see Figure 8*,* the longitudinal air stream directly affects the fire plume and the air velocity is increased until critical conditions are reached. However when there is a relatively large blockage ratio, see Figure 9*,* the fire plume is protected against longitudinal air flows, the tunnel height then is reduced and the smoke quickly penetrates this zone, the air stream required to avoid the backlayering phenomenon is higher then since part of the air stream is blocked. This approach can explain why for certain fire position the critical velocity does no decrease when there is a vehicular blockage as expected or at least following the trend of the experimental data.

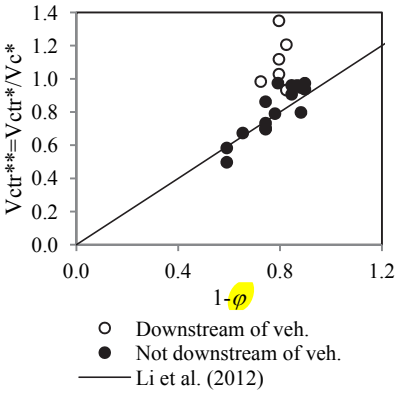

Figure 6 – Dimensionless critical velocity as a function of 1-φ. Data from experimental results.

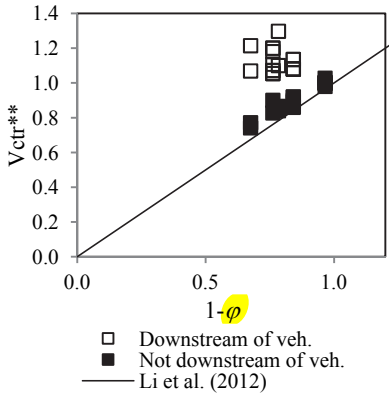

Figure 7 – Dimensionless critical velocity as a function of 1- φ. Data from Lee & Tsai study.

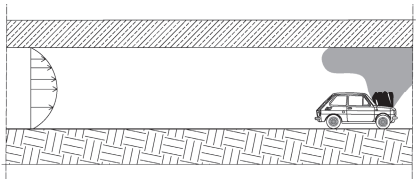

Figure 8 – Schematic of tunnel without vehicular blockage.

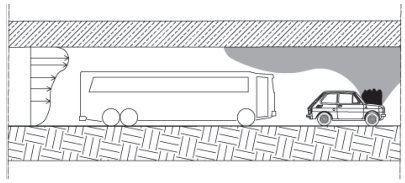

Figure 9 – Schematic of tunnel with vehicular blockage.

The obtained data regarding the backlayering distance in cased without vehicular blockage is plotted as a function of the confinement velocity in Figure 10, as well a reference correlation is plotted, see equation (8), which was defined by Li et al. [21]. It can be seen the obtained data are in good agreement with the reference correlation, although the data is in certain degree scattered around the reference curve but it shows the same trend. The fact that the data is scattered is due to the when performing the experiments the backlayering distance was not entirely steady, often it fluctuated ±4cm and this is due to the small throw produced the fog generator.

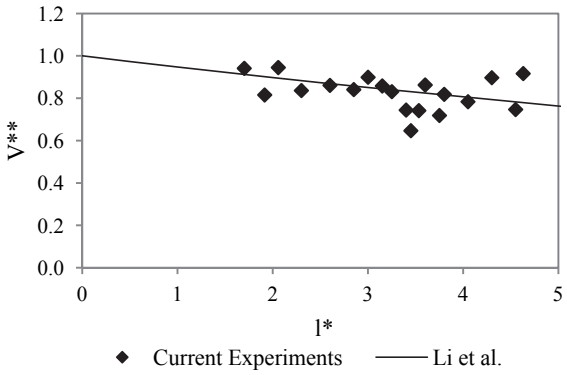

Figure 10 – Dimensionless backlayering distance as a function of the confinement velocity.

The backlayering distance was also measured when there was vehicular blockage inside the tunnel model. The data obtained which corresponds to several blockage ratios and fire source positions from the experiments can be seen in Figure 11 as a function of the confinement velocity, also a correlation proposed by Li et al. [21] is represented, equation (9), which corresponds to a vehicular blockage ratio of 20%, the correlation that was obtained based on data from experiments having the fire location located 4 cm. underneath the train model. As it can be seen the obtained data is not in agreement with the reference correlation, most of the data underestimate the reference correlation, in terms of vehicular blockage the obtained data lies between 10.3 to 41 %, whereas the reference correlation correspond to 20% blockage ratio, furthermore the relative position of the fire source during the experiments blocked or not the fire plume, thus the results cannot be compared against correlations. This suggests that the reference correlation cannot be extrapolated for other different conditions and blockage ratios. The blockage ratio then exerts an influence on the backlayering distance.

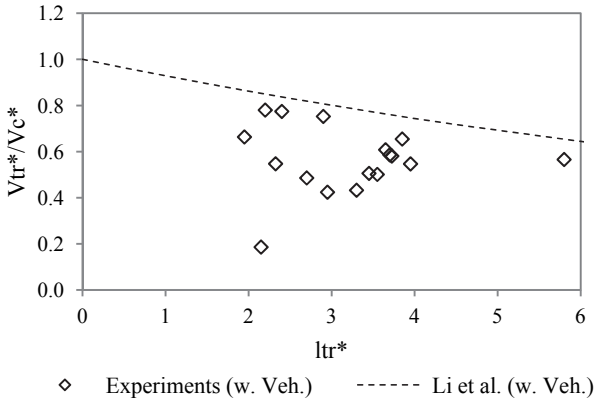

Figure 11 – Dimensionless backlayering distance as a function of the confinement velocity when there is vehicular blockage.

5. CONCLUSION

The tunnel model and the method used and presented in this article are able to reproduce several phenomena under different parametrical conditions and give semi-quantitative information. The experimental set-up enabled reproduction of the buoyancy phenomena to a certain extent, except for medium-large size HRR due to other factors (equipment), and has been partly validated.

The presence of vehicular blockage in tunnels can affect the critical velocity approximately as equal as the blockage ratio. But on the contrary the relative position of the buoyant injection/fire source and the relative size of the vehicular blockage can increase the critical velocity. When the buoyant jet is directly reached by the air flow, then the critical velocity decreases, but if it is partly blocked and the air flow does not reach it, then the critical velocity increases. Data from Lee & Tsai [23] with a thermal model, confirm this hypothesis. Furthermore Li et al.[21] and Wu & Bakar [14] results confirm that the critical velocity is reduced in the same range as the blockage ratio, However this is a semi-qualitative conclusion, no full-scale data has been reported in tunnel with blockage.

The tunnel model has been able to correlate well the dimensionless backlayering distance against a reference correlation, the data showed the same behaviour as the correlation proposed by Li et al.[21], although the data lies a bit scattered, that might be explained by human error.

The backlayering distance in tunnel with vehicular blockage has been studied by Li et al. [21], in their study they proposed a correlation for the dimensionless confinement velocity as function of the dimensionless backlayering distance when there is a vehicular blockage occupying 20% of the tunnel cross section. The obtained data do not correspond the aforementioned correlation, it might be due to the proposed model by Li et al. [21] cannot be used as a reference study inasmuch as the backlayering distance was based solely on one tunnel section and the fire source was placed 4 cm underneath the vehicular blockage. Further experiments are required in order to better observe possible behaviours.

The scaled tunnel model can be modulated and therefore it can be used to study a range of different scenarios, including the effect of tunnel inclination. Further experiments should be undertaken to fully understand the effect of vehicular blockage depending on the relative position to the fire source and the blockage ratio.

ACKNOWLEDGEMENT

The authors would like to acknowledge the help that O. Vauquelin and H. Ingason provided in the process and for their valuable input.

BIBLIOGRAPHY

[1] Flashback: Kaprun ski train fire 2004. http://news.bbc.co.uk/1/hi/world/europe/3502265.stm (accessed August 6, 2014).
[2] Land transport accident investigation bureau (BEA-TT) n.d. http://www.bea-tt.equipement.gouv.fr/_affiche_article.php3?id_article=33 (accessed August 6, 2014).
[3] Lönnermark A. On the Characteristics of Fires in Tunnels Doctoral Thesis. 2005.
[4] PIARC Committee on Road Tunnels. Maitrise des incendies et des fumees dans les tunnels routiers - Fire and Smoke control in road tunnels. PIARC Committee on Road Tunnels; 1999.
[5] Gaillot S, Revell a., Blay D, Vantelon J-, Deberteix P. Contribution To The Control Of Fire-induced Smoke Flow In Longitudinally Ventilated Tunnels. Fire Saf Sci 2005;8:1449–60. doi:10.3801/IAFSS.FSS.8-1449.
[6] Li YZ, Lei B, Ingason H. Theoretical and Experimental Study of Critical Velocity for Smoke Control in a Tunnel Cross-Passage. Fire Technol 2010;49:435–49. doi:10.1007/s10694-010-0170-0.
[7] Thomas PH. Modelling of Compartment Fires 1983;5:181–90.
[8] Thomas PH. The movement of smoke in horizontal passages against an air flow. Fire Res Stn 1968.
[9] Hinkley PL. A preliminary note on the movement of smoke in an enclosed shopping mall 1970.
[10] Heselden AJM. Studies of fire and smoke behaviour relevant to tunnels. Second Int. Symp. Aerodyn. Vent. Veh. Tunnels., Cambridge: 1976.

[11] Danzinger NH, Kennedy WD. Longitudinal ventilation analysis for the Glenwood Canyon tunnels. Aerodyn. Vent. Veh. Tunnels, York, U.K.: BHRA Fluid Engineering.; 1982.
[12] Vantelon JP, Guelzim A, Quach D, Kim Son D, Gabay D, Dallest D. Investigation of Fire-Induced Smoke Movement in Tunnels and Stations : An Application to the Paris Metro 1991:907–18.
[13] Oka Y, T G, Atkinson. Control of Smoke flow in Tunnel Fires 1996;25:305–22.
[14] Wu Y, Bakar MZA. Control of smoke flow in tunnel fires using longitudinal ventilation systems - a study of the critical velocity. Fire Saf J 2000;35:363–90. doi:10.1016/S0379-7112(00)00031-X.
[15] Kunsch JP. Simple model for control of fire gases in a ventilated tunnel. Fire Saf J 2002;37:67–81. doi:10.1016/S0379-7112(01)00020-0.
[16] Vauquelin O. Parametrical study of the back flow occurrence in case of a buoyant release into a rectangular channel. Exp Therm Fluid Sci 2005;29:725–31. doi:10.1016/j.expthermflusci.2005.01.002.
[17] Vauquelin O, Wu Y. Influence of tunnel width on longitudinal smoke control. Fire Saf J 2006;41:420–6. doi:10.1016/j.firesaf.2006.02.007.
[18] Ingason H, Lönnermark A, Li YZ. Model of ventilation flows during large tunnel fires. Tunn Undergr Sp Technol 2012;30:64–73. doi:10.1016/j.tust.2012.02.007.
[19] Deberteix P, Gabay D, Blay D. Experimental study of fire-induced smoke propagation in a tunnel in the presence of longitudinal ventilation. Proceeedings Int. Conf. Tunn. Fires Escape from Tunnels, Washington: 2001, p. pp. 257–65.
[20] Vauquelin O, Telle D. Definition and experimental evaluation of the smoke “confinement velocity” in tunnel fires. Fire Saf J 2005;40:320–30. doi:10.1016/j.firesaf.2005.02.004.
[21] Li YZ, Lei B, Ingason H. Study of critical velocity and backlayering length in longitudinally ventilated tunnel fires. Fire Saf J 2010;45:361–70. doi:10.1016/j.firesaf.2010.07.003.
[22] Li L, Cheng X, Cui Y, Li S, Zhang H. Effect of blockage ratio on critical velocity in tunnel fires. J Fire Sci 2012;30:413–27. doi:10.1177/0734904112443508.
[23] Lee Y-P, Tsai K-C. Effect of vehicular blockage on critical ventilation velocity and tunnel fire behavior in longitudinally ventilated tunnels. Fire Saf J 2012;53:35–42. doi:10.1016/j.firesaf.2012.06.013.
[24] Mégret O, Vauquelin O. A model to evaluate tunnel fire characteristics. Fire Saf J 2000;34:393–401. doi:10.1016/S0379-7112(00)00010-2.
[25] Megret O. Etude expérimentale de la propagation des fumées d’incendie en tunnel pour différents systénes de ventilation," PhD Thesis. University of Valencienne, France, 1999.
[26] Megret O, Vauquelin O. A reduced scale tunnel for the study of fire-induced smoke control. 1998.
[27] Quintiere J. Scaling applications in fire research. Fire Saf J 1989;15:3–20.
[28] Vauquelin O, Michaux G, Lucchesi C. Scaling laws for a buoyant release used to simulate fire-induced smoke in laboratory experiments. Fire Saf J 2009;44:665–7. doi:10.1016/j.firesaf.2008.11.001.
[29] Hiroshi K, Taro Y. Air entrainment and thermal radiation from heptane pool fires. Fire Technol 1988;24:33–47. doi:10.1007/BF01039639.
[30] Ingason H, Zhen Li Y, Lönnermark A. Tunnel Fire Dynamics. BORÅS, Sweden: Springer; n.d.

APPENDIX

Table A1 – Characteristics of the buoyant sources for tunnel with different heights in full scale and their corresponding values in 1/30 scale.

	Full-scale values								Reduced scale model								
	D	$\dot{Q}$	Tunnel height 4.5 m.		Tunnel height 6 m.		Tunnel height 10.5 m.		D	Tunnel height 4.5m.			Tunnel height 6m.			Tunnel height 10.5		
Source nr.	[m]	[MW]	T_s [K]	q_s [m^3/s]	T_s [K]	q_s [m^3/s]	T_s [K]	q_s [m^3/s]	[mm]	X_{he}	q_{air} [l/min]	q_{he} [l/min]	X_{he}	q_{air} [l/min]	q_{he} [l/min]	X_{he}	q_{air} [l/min]	q_{he} [l/min]
1	0.62	0.42	520	1.89	490	2.06	441	2.50	21	0.50	11.6	11.4	0.45	13.7	11.4	0.38	18.98	11.4
2	0.78	0.78	548	3.31	514	3.61	460	4.33	26	0.53	18.9	21.3	0.49	22.5	21.4	0.41	31.26	21.5
3	0.84	0.96	558	3.96	522	4.31	466	5.16	28	0.54	22.1	26.0	0.50	26.3	26.1	0.42	36.61	26.2
4	1.02	1.61	585	6.30	546	6.83	484	8.13	34	0.57	33.0	43.6	0.53	39.4	43.8	0.44	54.96	44.0
5	1.23	2.62	614	9.77	571	10.57	503	12.50	41	0.60	48.0	71.0	0.55	57.4	71.3	0.47	80.36	71.8
6	1.62	5.28	662	18.33	612	19.73	534	23.10	54	0.64	81.0	142.1	0.59	97.3	142.8	0.51	137.22	144.0
7	1.8	6.85	681	23.16	629	24.89	547	29.04	60	0.65	98.1	183.9	0.61	118.0	184.9	0.53	167.00	186.5
8	2.07	9.60	709	31.42	654	33.69	566	39.11	69	0.67	125.4	257.1	0.63	151.4	258.6	0.55	215.06	261.0
9	2.4	13.61	741	43.06	681	46.06	587	53.21	80	0.69	160.9	363.2	0.65	194.9	365.6	0.57	278.37	369.3
10	2.59	16.24	758	50.50	696	53.94	598	62.17	86	0.70	182.2	432.5	0.66	221.2	435.4	0.58	316.67	440.0
11	2.79	19.24	775	58.88	712	62.82	610	72.22	93	0.71	205.1	511.5	0.67	249.5	515.2	0.59	358.22	520.8
12	3.2	26.16	809	77.7					80	0.73	123.3	337.5						
13	3.45	30.87	828	90.3					86	0.74	137.9	397.4						